Multiple-Particle Tracking Measurements of Heterogeneities in Solutions of Actin Filaments and Actin Bundles

Joshua Apgar,* Yiider Tseng,* Elena Fedorov,† Matthew B. Herwig,* Steve C. Almo,† and Denis Wirtz*‡
Departments of *Chemical Engineering and ‡Materials Science and Engineering, The Johns Hopkins University, Baltimore, Maryland 21218; and †Department of Biochemistry, Albert Einstein College of Medicine, Yeshiva University, Bronx, New York 10461 USA

ABSTRACT One of the central functions of actin cytoskeleton is to provide the mechanical support required for the establishment and maintenance of cell morphology. The mechanical properties of actin filament assemblies are a consequence of both the available polymer concentration and the actin regulatory proteins that direct the formation of higher order structures. By monitoring the displacement of well-dispersed microspheres via fluorescence microscopy, we probe the degree of spatial heterogeneity of F-actin gels and networks in vitro. We compare the distribution of the time-dependent mean-square displacement (MSD) of polystyrene microspheres imbedded in low- and high-concentration F-actin solutions, in the presence and absence of the F-actin-bundling protein fascin. The MSD distribution of a 2.6-μM F-actin solution is symmetric and its standard deviation is similar to that of a homogeneous solution of glycerol of similar zero-shear viscosity. However, increasing actin concentration renders the MSD distribution wide and asymmetric, an effect enhanced by fascin. Quantitative changes in the shape of the MSD distribution correlate qualitatively with the presence of large heterogeneities in F-actin solutions produced by increased filament concentration and the presence of actin bundles, as detected by confocal microscopy. Multiple-particle tracking offers a new, quantitative method to characterize the organization of biopolymers in solution.

INTRODUCTION

Changes in cell migration, morphology, adhesion, and growth depend on the dynamic reorganization of the actin cytoskeleton, a highly integrated array of interconnected filament assemblies (Lauffenburger and Horwitz, 1996). Actin regulators direct the assembly of complex structures (Small et al., 1999), including focal adhesions (Tamura et al., 1998), dendritic actin networks at the cell's leading edge (Svitkina and Borisy, 1999), stress fibers (Furukawa and Fecheimer, 1996), lamellipodia (Mitchison and Cramer, 1996), and filipodia (Miki et al., 1998). Depending on the type of cell and tissue, the organization of these different actin assemblies may be controlled by extracellular ligands such as growth factors and hormones (Hall, 1998; Clark and Brugge, 1995), by the chemical and physical nature of the extracellular matrix (Hynes, 1989; Palecek et al., 1998; Pelham and Wang, 1997), and by mechanical forces such as those exerted by blood flow (Konstantopoulos and McIntire, 1996). These various actin assemblies ultimately modulate the viscoelastic properties of the cytoplasm, which regulate cell-shape changes to allow for cellular activities such as cytokinesis and cell locomotion (Janmey, 1998; Luby-Phelps, 1993).

Similarly, the structure of an actin filament network in vitro determines its viscoelastic properties: the stiffness of a semidilute solution of filamentous actin (F-actin) is proportional to the inverse of the entanglement length (Morse, 1998a). Polymer models (Morse, 1998a,b,c; Gittes and MacKintosh, 1998; Isambert and Maggs, 1996; Kroy and Frey, 1996), which correctly predict this result, implicitly assume that the solution mesh size is uniform. This assumption has been validated for un-cross-linked F-actin at equilibrium (Morse, 1998a); however, such an assumption may not be correct for F-actin networks with quenched disorder, such as those created by cross-linking and/or bundling proteins during gelation. Local variations in the mesh size of the F-actin network may result in global effects on its viscoelastic properties. Even in the absence of actin-binding proteins, solutions of F-actin may display large, local variations of microstructure. For instance, in the early phase of gelation, the non-uniformity of the F-actin network may cause the slow increase of the global stiffness of F-actin network until the mesh size becomes more uniform (Xu et al., 1998a).

The spatial arrangement of actin polymers in vitro is often assessed by electron microscopy (EM) or fluorescent microscopy (Mullins et al., 1998; Carlier et al., 1997). EM has been used extensively to probe the helical structure of individual actin filaments in both the presence and absence of actin-binding proteins (Hanein et al., 1998; Owen et al., 1996). Using negative staining, EM can also readily identify the presence of actin bundles that are formed by actin-binding proteins (Milligan and Flicker, 1987; Sasaki et al., 1996; McGough et al., 1998). With negative staining, actin filaments form a highly congested network and become indistinguishable from each other at concentrations as low

Received for publication 22 December 1999 and in final form 22 April 2000.

J. A. and Y. T. contributed equally to this work.

Address reprint requests to Denis Wirtz, Ph.D., Department of Chemical Engineering, The Johns Hopkins University, 3400 N. Charles St., Baltimore, MD 21218. Tel.: 410-516-7006; Fax: 410-516-5510; E-mail: wirtz@jhu.edu.

0006-3495/00/08/1095/12 $2.00

as 2 μM, lower than those necessary to make a F-actin solution elastic ($\approx$5 μM) (Palmer et al., 1999) and much lower than physiological concentrations of actin ($\approx$200–300 μM). Moreover, EM often requires invasive staining of the specimen, which may affect macromolecular interactions and influence filament organization and does not preserve the organization of the network upon buffer evaporation during specimen preparation. The integrity of the actin network can be preserved by freeze etching and/or sectioning, but a quantitative method to extract the network's degree of heterogeneity from EM images has yet to be implemented.

Fluorescence microscopy permits the study of actin filaments in an aqueous environment, and therefore better preserves the three-dimensional nature of an F-actin network. However, the limited spatial resolution of light microscopy does not allow for the examination of the heterogenehity of a concentrated solutions of overlapping polymers (Kas et al., 1996). Diffraction-limited images of fluorescently labeled actin filaments and bundles containing few filaments are indistinguishable. Therefore, although fluorescence microscopy can readily detect the presence of large actin bundles and aggregates in concentrated solutions, it is unsuitable to quantify the spatial organization and internal structure of an actin filament network.

We describe an approach that monitors the displacements of a large ensemble of individual well-dispersed microspheres in a concentrated actin filament solution to assess the degree of heterogeneity of that solution. Recent advancements in microscopy, spectroscopy, and image processing allow for the displacements of particles to be tracked in solution with sub-micron resolution. For instance, diffusing wave spectroscopy (DWS) probes the motion of several thousands of particles simultaneously with subnanometer spatial resolution and microsecond temporal resolution (Palmer et al., 1998b, 1999). DWS allows for the collection of very low-noise mean-square displacement (MSD) spectra, from which rheological data can be generated over a wide frequency range. However, much information is lost because DWS measurements are intrinsically ensemble-averaged, and hence, cannot be used to measure the MSD distribution. Single-particle tracking, using either video-enhanced light microscopy (Mason et al., 1997a) or laser deflection (Mason et al., 1997b; Gittes et al., 1997; Schnurr et al., 1997), has been an effective approach to measure the lateral diffusion of proteins in plasma membrane (Kusumi and Sako, 1996; Edidin et al., 1991) and the local microrheology of cytoplasm and plasma membrane of living cells (Lee et al., 1993; Yamada et al., 2000). Because single-particle tracking monitors the displacement of one microsphere at a time, it is a relatively inefficient and time-consuming method for the generation of ensemble-average MSDs and MSD distributions over a whole specimen (Qian et al., 1991).

We track a large number of individual fluorescently-labeled microspheres to quantify the spatial organization of F-actin solutions. The distribution of particle displacements showed a significant dependence on the types of actin structures present in solution. We found that in addition to differences in the magnitude of the ensemble-averaged MSD, the MSD distributions for a large ensemble of probed microspheres were similar for a glycerol solution and a low-concentration F-actin solution, but qualitatively different from a high-concentration F-actin solution and a solution of bundled F-actin. The implementation of image-processing software allowed for fast, convenient, and quantitative multiple-particle tracking (MPT) measurements. These MPT studies provide a strong complement to traditional biophysical methods (rheology, microscopy, spectroscopy, and light scattering) for the characterization of the properties of actin filament networks in vitro. This information begins to provide the basis for understanding the in vivo mechanics of actin filament function.

METHODS AND MATERIALS

Protein preparation

Unless specified, all reagents were purchased from Sigma (St. Louis, MO). Actin was purified from chicken skeletal acetone powder by the method of Spudich and Watt (1971), followed by gel filtration on Sephacryl S-300 HR (MacLean-Fletcher and Pollard, 1980). The purified actin was stored as Ca^{2+}-actin in continuous dialysis at 4°C against buffer G (0.2 mM ATP, 0.5 mM dithiothreitol (DTT), 0.2 mM $CaCl_2$, 1 mM sodium azide, and 2 mM Tris-Cl, pH 8.0). The actin used in these studies was never frozen and was used within 5 days after preparation (Xu et al., 1998b). The final actin concentration was determined by ultraviolet absorbance at 290 nm, using an extinction coefficient of $2.66 \times 10^4\ M^{-1}cm^{-1}$ and a cell path length of 1 cm. Mg^{2+} -actin filaments were generated by adding 0.1 volume of 10-X KMEI (500 mM KCl, 10 mM $MgCl_2$, 10 mM EGTA, 100 mM Imidazole, pH 7.0) polymerizing salt buffer solution to 0.9 volume of G-actin in buffer G.

Human fascin was expressed as a glutathione s-transferase (GST) fusion using pGEX2T (Amersham Pharmacia, Piscataway, NJ) in the *Escherichia coli* strain JR600. Cultures were grown at 37°C to an OD_{600} of 0.6. After cooling to 25°C, 1 mM isopropylβ-D-thiogalactopyranoside was added and growth continued overnight. Cells were harvested by centrifugation, washed with PBS, and resuspended in PBS containing 1 mM DTT and 0.2 mM phenylmethylsulfonyl fluoride. Cells were disrupted by sonication and the lysate clarified by centrifugation in a SS-34 rotor (Sorvall, Newtown, CT) at 15,000 rpm for 20 min. The lysate was applied to a glutathione-Sepharose column equilibrated in PBS containing 1 mM DTT (PBS/DTT). The column was washed extensively and the fusion protein eluted with 10 mM glutathione, 50 mM Tris, pH 8.0, 1 mM DTT, and 0.1 M NaCl. The fusion protein was dialyzed against PBS/DTT and fascin was liberated from glutathione S-transferase by cleavage with thrombin, followed by glutathione-Sepharose chromatography. The fascin was dialyzed against 10 mM Tris and 1 mM DTT, pH 8.0, and applied to a DE52 column that was developed with a linear gradient of 0 to 70 mM NaCl in 10 mM Tris, pH 8.0, and 1 mM DTT. Purified fascin was dialyzed against 10 mM Tris, pH 8.0, 10 mM NaCl, 30 mM KCl, 0.1 mM EDTA, and 1 mM DTT and stored at −70°C.

Glycerol and actin solutions

Aqueous (1% vol water) solutions of glycerol and a bead stock solution (Bioclean beads, 1.04 μm mean diameter, 1% Solids, Duke Scientific, Palo

Alto, CA) were combined and homogenized by vortexing the solution for 15 min. The solution was allowed to equilibrate overnight at 4°C. For experiments in actin, a homogeneous solution of beads was added to the actin solution and was briefly vortexed, followed by the addition of 10-X KMEI to induce polymerization. The solution was allowed to gel overnight at 4°C. MPT measurements described below were found to be independent of gelation time after 6 h for actin solutions in the absence of fascin, in agreement with published rheological measurements that show that the F-actin solution is equilibrated after 6 h (Xu et al., 1998a). The same protocol was followed for the actin solutions with fascin, but, following published protocols (Sasaki et al., 1996), the solution was allowed to incubate at 4°C for 8 days so as to probe the solution at equilibrium.

Sample holder assembly and data collection

Twenty microliters of sample were loaded into PC20 CoverWell (Grace Bio-Lab, Eugene, OR) and carefully covered with a glass coverslip to avoid trapping any air bubbles. The self-sealing assembly was further sealed with quick-drying boat sealer and then attached to a glass microscope slide with double-sided tape. The sample holder was loaded onto a Nikon upright epifluorescence microscope with 100× oil-immersion lens (N.A. 1.3; Nikon, Inc., Melville, NY). The sample was maintained at room temperature for 2 h to allow the system to come to equilibrium and the gel to completely relax. This was confirmed, before the characterization of each sample, by tracking particles for 1000 s and checking for a net motion of the particles over this time interval. Once the sample had relaxed, the trajectories of particles were recorded using a VE-1000 SIT Camera (Dage-MTI, Michigan City, IN) mounted on the microscope and a digitizer board (Data Translation, Marlboro, MA) installed in a PowerMacintosh 7200 computer (Apple Inc., Sunnyvale, CA), as described (Leduc et al., 1999). Frames were captured for 100 s at a rate of 10 frames/s; fields of view were selected at random, and the total number of tracked particles per sample ranged between 250 and 350. To minimize the effect of particle-particle interactions, beads that were less than 10 bead-diameters apart from neighboring beads were excluded. Importantly, the exclusion of particles that were close to each other also greatly improved the reliability of the matching protocol described below. To minimize bead-coverslip interactions and not to track beads that had fallen to the bottom of the microscopy chamber, the microscope was focused to the mid-height of the sample, ≈50 μm away from the coverslip.

Multiple-particle tracking

Images of the probe microspheres were acquired with NIH Image (National Institutes of Health, Bethesda, MD) and segmented using a custom-made routine that incorporated the NIH Image commands Threshold and Analyze Particles. Threshold works by segmenting the beads from the background based on the intensity values. Analyze Particles finds the center of each particle by tracing the edge of each bead and computing its centroid. The bead positions were matched frame by frame, using a custom-made routine incorporated into NIH Image, to identify each particle and generate its trajectory. Frame-by-frame matching assumes that the closest particle in the next frame is the same particle. This is a reasonable assumption because the change in position from frame to frame was very small compared to the spacing between beads (see Results). Particle-matching allowed us to track between 5 and 10 beads simultaneously, which greatly improved statistics and reduced times of movie-capture compared to single-particle tracking (Mason et al., 1997b,a). Although MPT can track an even larger number of particles, we did not increase the number of probe particles to avoid particle-particle interactions and to avoid artifactual geometric deformation of the fluorescent trace of a given particle in focus by fluorescent particles out of focus. From the particle trajectories, another routine incorporated into NIH Image produced a MSD-versus-time scale curve for each particle.

We ensured that the shape of the MSD distribution was independent of bead size by conducting MPT measurements with probing beads of various bead diameters (1.2 μm, 0.85 μm; data not shown). It is important to note that the diameter of the beads used in the experiments was larger than the mesh size of the actin solution (Luby-Phelps et al., 1987; Jones and Luby-Phelps, 1996). Hence, for the scales smaller than 1000 s, our particles did not percolate through the network, as the displacements of the probing microspheres were found to be equal or smaller than the microsphere diameter (see Results and Discussion). We also found that the viscoelastic properties of F-actin gels calculated from MSD measurements and measured directly by rheometry were similar (Palmer et al., 1999; see Results). This strongly supported the assumptions that beads interacted only sterically with F-actin and that polystyrene microspheres did not induce the formation of a depletion zone in the microsphere vicinity.

Confocal fluorescence microscopy

To prepare F-actin for fluorescence microscopy, 10 μl of 6.6 μM rhodamine phalloidin (Molecular Probes, Eugene, OR) in methanol was deposited on a microscopy PC20 CoverWell chamber and allowed to dry for 1 hour. One volume of 10× KMEI/fluorescence buffer containing 500 mM KCl, 10 mM $MgCl_2$, 10 mM EGTA, 100 mM Imidazole (pH 7.0), as well as 1 M DTT, 0.18 mg/ml catalase, 1 mg/ml glucose oxidase, and 30 mg/ml glucose, was added to 9 volumes of actin solution to polymerize actin and reduce photobleaching of rhodamine phalloidin. The coverslip was mounted on a glass slide, and polymerization was allowed to proceed overnight. Samples were observed with a Nikon PCM 2000 laser-scanning confocal system attached to a Nikon TE300 inverted microscope using a 100× oil-immersion objective (N.A. 1.3). Twenty optical sections separated by 0.5 μm were captured in series and combined to generate maximum projections of the actin gels using the software SimplePCI (Compix, Cranberry Township, PA). The actin and fascin concentrations used for confocal microscopy were the same as those used for multiple-particle tracking (MPT).

RESULTS

MPT in a homogeneous viscous solution

Using MPT, we monitored the trajectories of 1.04 μm-diameter polystyrene microspheres suspended in an aqueous solution of glycerol. Glycerol was selected because it is a purely viscous fluid (i.e., elastic modulus is zero) and because its shear viscosity, $\eta \approx 1$ Poise, was close to that of the actin solutions tested below (Xu et al., 1998c,a). At length scales comparable to the size of the microsphere, the glycerol solution does not display any microstructure, and can be considered to be perfectly homogeneous. We were able to probe displacements as small as ≈4 nm, as determined by immobilizing 1.04 μm-diameter microspheres on microslides using a strong adhesive (Loctite, Newington, CT) and tracking their apparent displacement. This outstanding spatial resolution allowed us to measure the displacement of microspheres in liquids of high viscosity (see Fig. 1 *a*), for which microspheres diffusion was more restrained than in a low-viscosity liquid. High viscosity also had the advantage of maintaining the fluorescent microspheres in the field of focus of the microscope for extended periods of time. For each sample, we verified that the solution did not undergo any convection such as those

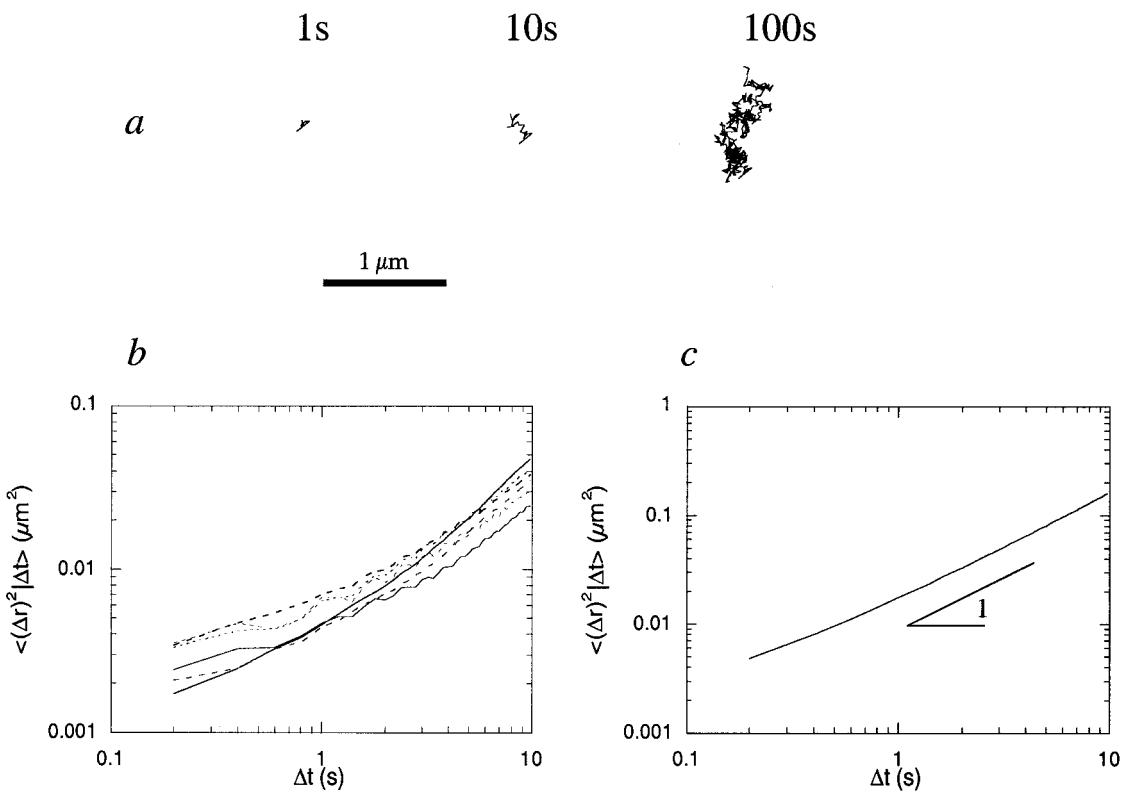

FIGURE 1 Trajectory and associated mean square displacement (MSD) of microspheres in glycerol. Polystyrene microspheres (1.04 μm diameter) are suspended at a volume fraction of 0.1% in an aqueous solution of glycerol, which has a shear viscosity of $\approx$1 Poise. (*a*) Typical trajectory of one microsphere at 1s, 10s and 100s time scales. (*b*) Randomly selected MSDs of individual microspheres. (*c*) Ensemble-average MSD (n = 350). MSD increases proportionally to time, as expected for a purely viscous fluid.

generated by capillary effects, by monitoring the long time-scale displacement ($t > 1000$ s), and testing for possible correlation of the displacement of distant particles. We selected MPT experiments for which no such correlation was observed. For each trajectory, exploiting time invariance, the mean-square displacement (MSD) was calculated as a function of time scale Δt (see Fig. 1 *b*). Finally, the ensemble-average mean square displacement of a large number of microspheres was computed (see Fig. 1 *c*), from which the average solution viscosity, η, could be extracted, since MSD is given in two dimensions by $\langle \Delta r^2(t) \rangle = 4D\Delta t$. Here, $D = k_BT/6\pi\eta a$ is the microsphere diffusion coefficient, k_B is Boltzmann's constant, T is the absolute temperature, and a is the particle radius. The viscosity calculated from the ensemble-average MSD was $\eta \approx 1.02$ Poise, close to the nominal viscosity.

MPT in F-actin solutions in the presence/absence of human fascin

The trajectories of microspheres in an F-actin solution were monitored in the presence and in the absence of the F-actin bundling protein fascin. In the absence of fascin, the extent of microsphere displacement was greatly decreased with increasing actin concentration (Fig. 2, *a* and *b*). As shown previously (Palmer et al., 1999), this decrease in the magnitude of particle displacement corresponded to an increase in the stiffness of the actin network. Trajectories of microspheres dispersed in a high-concentration actin solution were slightly more heterogeneous in amplitude than in a low-concentration actin solution (see further details below). This effect was greatly enhanced in the presence of fascin, which resulted in two populations of MSDs that corresponded to (a majority of) microspheres that moved little and (a minority of) microspheres that moved exceedingly large distances (Fig. 2, *c* and *c′*).

MSDs were extracted from measured displacements (Fig. 3, *a*, *c*, and *e*), which allowed for the computation of the associated ensemble-average MSDs (Fig. 3, *b*, *d*, and *f*). The temporal dependence and the magnitude of the ensemble-average MSD varied with actin concentration and the presence/absence of fascin. Such observations were qualitatively similar to those reported previously for F-actin solutions and F-actin in the presence of the actin cross-linking protein α-actinin (Palmer et al., 1998b, 1999; Xu et al., 1998d). Using the measured ensemble-average MSDs, $\langle \Delta r^2 \rangle$, the plateau modulus of the F-actin solutions can be approximately estimated by $G \approx 2k_BT/3\pi a\langle \Delta r^2 \rangle$ (Mason

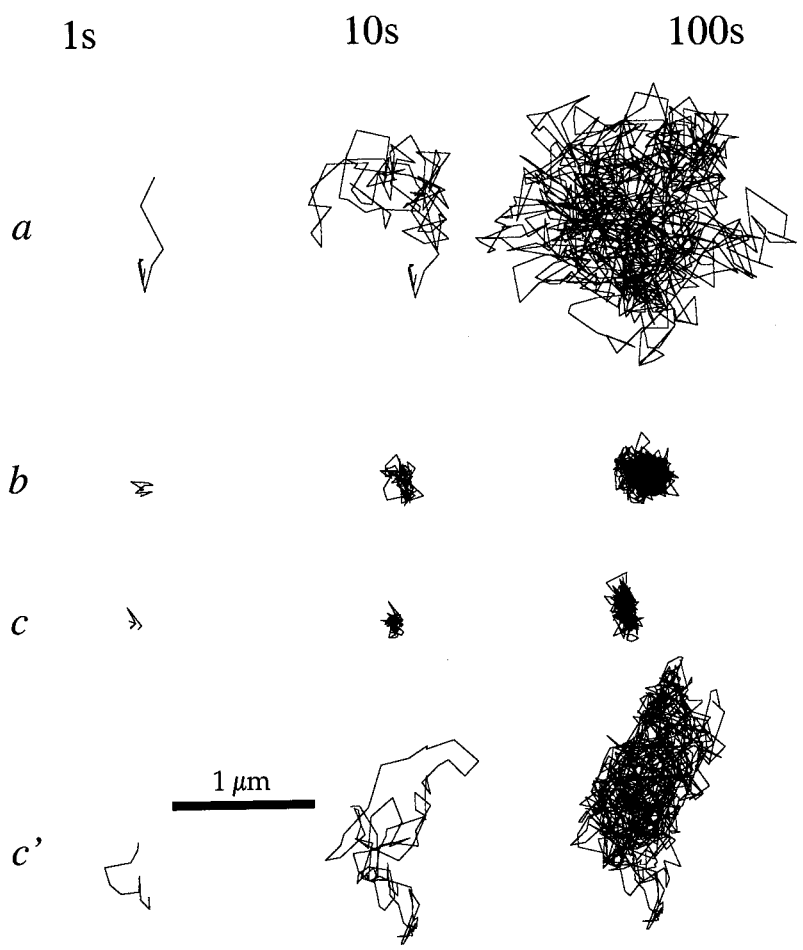

FIGURE 2 Trajectories of one microsphere in a low-concentration F-actin solution and a high-concentration F-actin solution in the presence and the absence of the F-actin-bundling protein fascin. Trajectories are shown for a 1-, 10-, or 100-s time span. (*a*) 2.6 μM F-actin. (*b*) 26 μM F-actin. "Tight" (*c*) and "loose" (*c'*) trajectories in a solution containing 26 μM F-actin and 0.26 μM fascin. See text for more details.

and Weitz, 1995; Mason et al., 1997b). The measured ensemble-average MSDs, estimated at $\Delta t = 1$ s, are $\langle \Delta r^2 \rangle \approx 0.32\ \mu m^2$ and $0.02\ \mu m^2$ (see Fig. 3, *b* and *d*), for the 2.6 μM F-actin solution and the 26 μM F-actin solution, respectively. Hence, the corresponding plateau moduli are $G \approx 0.05$ dyn/cm^2 and 1.1 dyn/cm^2, respectively, which are somewhat smaller than G determined from rheometric analysis (Palmer et al., 1999; Xu et al., 1998a,b; Hinner et al., 1998). This may be due to the (very) approximate nature of the above formula for G. Note, however that these two measured values of G are compatible with the concentration-dependence of G, $G(c) \propto c^{7/5}$, predicted by Morse (1998b,c), Gittes and MacKintosh (1998), and Isambert and Maggs (1996), and already verified experimentally by Xu et al. (1998a) and Hinner et al. (1998). More importantly for the present paper, we found that the range of displacements at a given time scale was narrow for glycerol and 2.6 μM F-actin, became wider for 26 μM F-actin, and extremely wide for 26 μM F-actin in the presence of 0.26 μM fascin, respectively (see Fig. 3, *a*, *c*, and *e*).

The ranges of displacements were quantified by generating MSD distributions from measured MSDs of individual microspheres as a function of time and for each specimen. To focus on the range of MSD values as opposed to the magnitude of the MSD, we normalized MSD distributions with the corresponding ensemble-average MSD. At a fixed time scale (for instance $\Delta t = 2$s, see Fig. 4), as expected for an homogeneous viscous liquid, the MSD distribution for glycerol was tight and symmetric around the mean (Fig. 4 *a*). By contrast, the MSD distributions of F-actin solutions became wider and more asymmetric for increasing actin concentration and in the presence of fascin (Fig. 4, *b-d*). We also found that the MSD distribution for glycerol was approximately independent of time (Fig. 5 *a*), whereas the MSD distributions for the F-actin solutions with and without fascin became more skewed and broader for increasing time scales (Fig. 5, *b-d*).

MSD distributions, normalized by the mean, were analyzed by computing their median, standard deviation, skewness, maximum, and minimum values. We found that the median normalized by the (time-dependent) mean was approximately unity for glycerol and 2.6 μM F-actin, whereas the normalized median became lower than unity for 26 μM F-actin (0.91 at $\Delta t = 1$ s, 0.75 at $\Delta t = 10$ s). This trend was enhanced in the presence of fascin as the median decreased to values as low as 0.4 at $\Delta t = 10$ s (Fig. 6 *a*). The standard

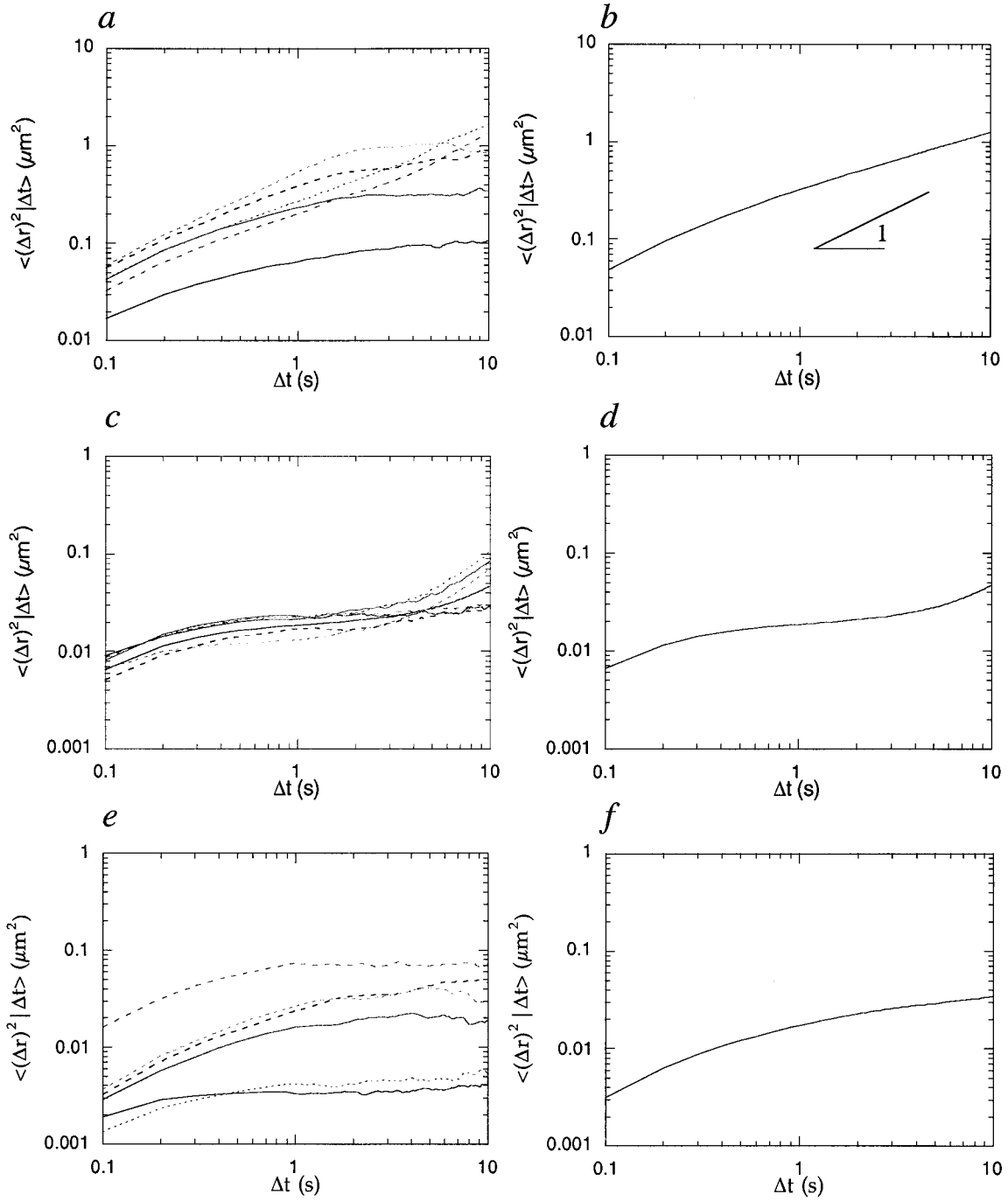

FIGURE 3 Individual MSDs and ensemble-averaged MSDs of microspheres dispersed (0.1% volume fraction) in a low-concentration actin solution and in a high-concentration F-actin solution in the presence and absence of fascin. (*a*), (*c*), and (*e*): Randomly selected MSDs of individual, 1.04 μm-diameter microspheres. (*b*), (*d*), and (*f*): Ensemble-average MSD ($250 < n < 400$). (*a*) and (*b*) 2.6 μM F-actin. (*c*) and (*d*) 26 μM F-actin. (*e*) and (*f*) 26 μM F-actin and 0.26 μM fascin.

deviation, the skewness, and the spread between maximum and minimum values of the normalized MSD distributions were generally higher for the F-actin with and without fascin than for glycerol (Fig. 6, *b-d*). In particular, the standard deviation was very low for glycerol, increased for F-actin solutions, and became extremely high in the presence of fascin. The minimum (and maximum) values of the MSD distribution measured at $\Delta t = 1$ s were relatively independent of actin concentration but strongly decreased (increased) in the presence of fascin compared to the uni-

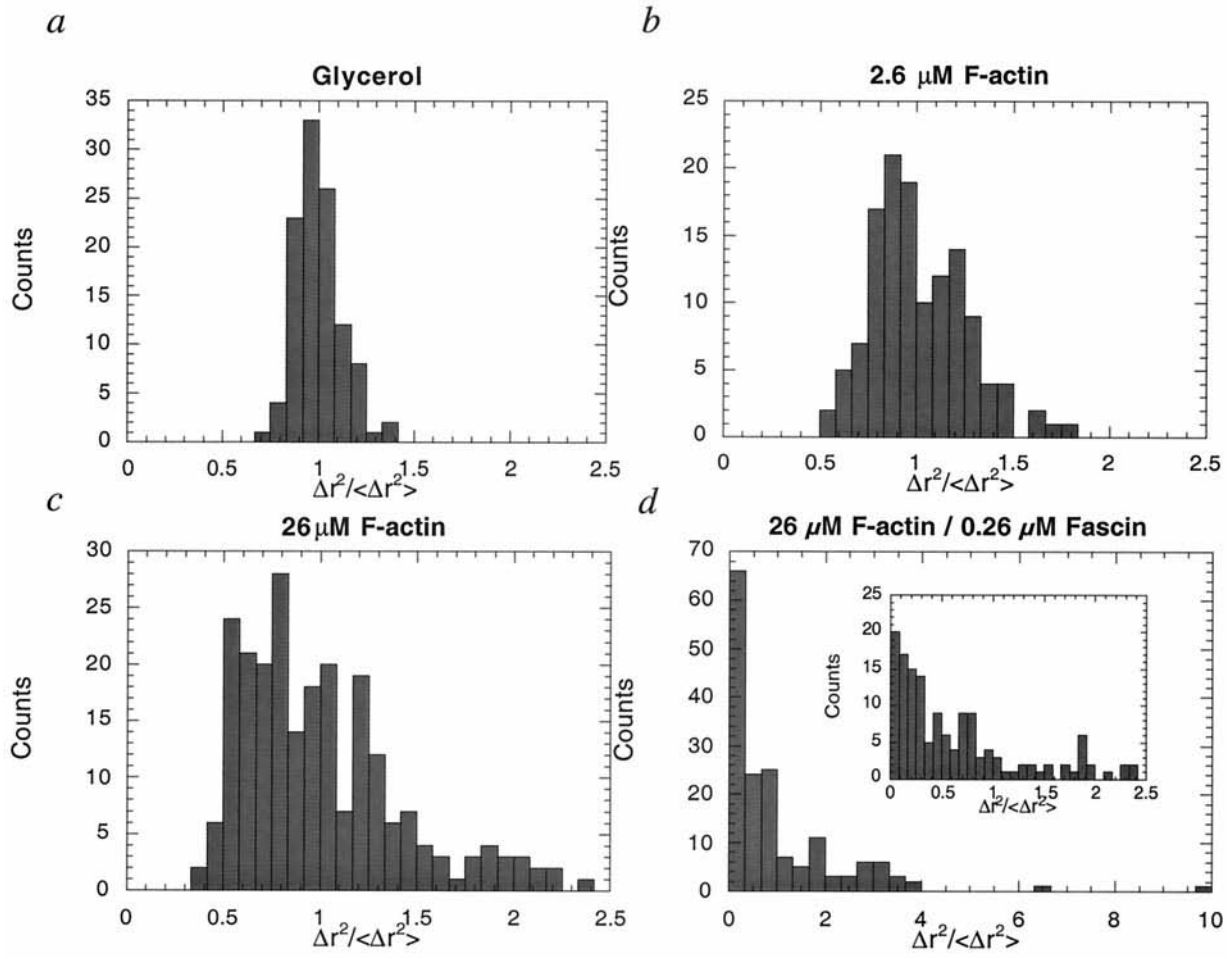

FIGURE 4 Distributions of the MSD of microspheres collected at time $\Delta t = 2$ s. MSD distributions are normalized by the ensemble-average MSD at each time scale and for each type of solution. (*a*) Glycerol. (*b*) 2.6 μM F-actin. (*c*) 26 μM F-actin. (*d*) 26 μM F-actin and 0.26 μM fascin. *Inset* in (*d*): MSD distribution for small deviations of the MSD with respect to the mean, $\langle \Delta r^2(t) \rangle$, to facilitate the comparison between *a* and *c*.

form solution of glycerol (Fig. 6 *b*). The skewness of the MSD distribution for glycerol was just slightly lower than that of the low-concentration F-actin solution, and hardly increased with actin concentration, but was strongly enhanced in the presence of fascin (Fig. 6 *c*). Standard deviation, skewness, and median were relatively independent of time scale for glycerol. With the exception of the standard deviation, these parameters were approximately independent of time scale for F-actin at low concentration as well, but became increasingly dependent on time scale for increasing actin concentration and in the presence of fascin (Fig. 6, *b-d*).

Confocal microscopy

Confocal microscopy was used to relate observed differences in MSD distributions with gross microstructural features among various actin solutions. We found that, due to the absence of large aggregates, a 2.6-μM solution of actin filaments displayed a relatively uniform distribution in orientation and spatial arrangement throughout the specimen (Fig. 7 *b*). A 26-μM solution of actin filaments instead exhibited relatively anisotropic features presumablly due to the intrinsic rigidity of actin filaments, which aligned one another via steric interactions (Fig. 7 *a*). Even at molar ratios as low as 1:100, fascin induced the formation of large bundles. Correspondingly, we found long anisotropic fluorescent spots, which correspond to F-actin bundles (Fig. 7 *c*; Sasaki et al., 1996). These bundles were surrounded by zones relatively depleted of F-actin.

DISCUSSION

Correlation between actin structures present in solution and MSD distribution

In vivo and in vitro studies have shown that the three major filamentous networks of the cytoskeleton in non-muscle

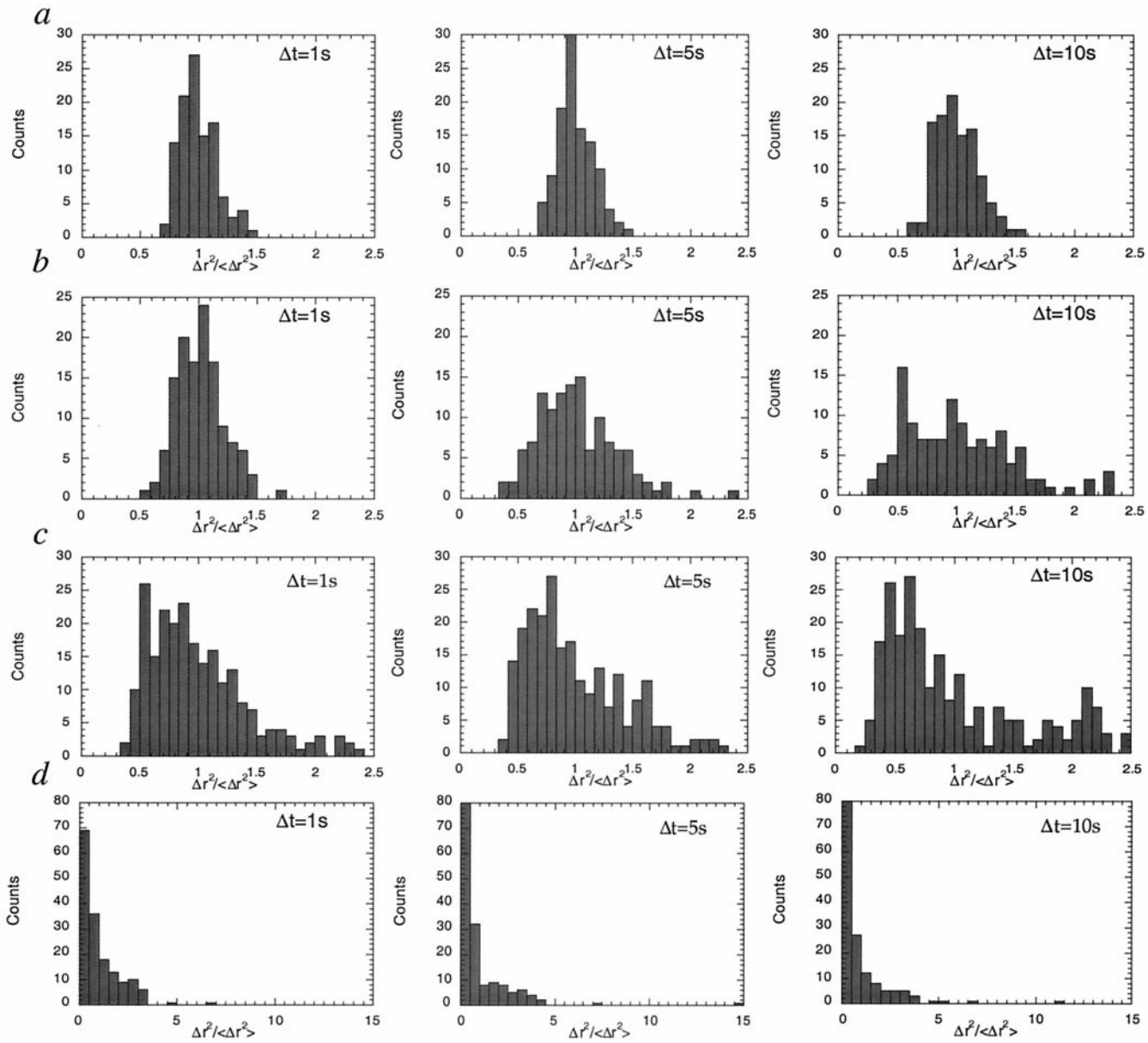

FIGURE 5 Time-dependent distributions of the MSD of microspheres suspended in glycerol, in a F-actin solution, and in a solution of F-actin and fascin. MSD distributions are normalized by the ensemble-average MSD, $\langle \Delta r^2(t) \rangle$, at each time scale and for each type of solution (see Fig. 3, *b*, *d*, and *f*). (*a*) Glycerol. (*b*) 2.6 μM F-actin. (*c*) 26 μM F-actin. (*d*) 26 μM F-actin and 0.26 μM fascin. First column, $\Delta t = 1$ s; second column, $\Delta t = 5$ s; third column, $\Delta t = 10$ s.

cells, actin filaments, intermediate filaments, and microtubules, form heterogeneous (i.e., non-constant mesh size) networks (Mullins et al., 1998; Wachsstock et al., 1993; Paladini et al., 1996; McGowan and Coulombe, 1998; Maciver et al., 1991; Tilney et al., 1995). Based on classical models of polymer physics (Morse, 1998a; Doi and Edwards, 1989), it is expected that these microstructural heterogeneities will modify the mechanical properties of a cytoskeleton network. Using multiple-particle tracking, we found that the MSD distribution of microspheres dispersed in various types of F-actin solutions is qualitatively different from that of a homogeneous solution (glycerol). MSD distributions exhibited a strong dependence on actin concentration and was very sensitive to the presence of the F-actin bundling protein human fascin. The median of the MSD distribution was found to decrease and the skewness and standard deviation to increase with increasing actin concentration and this trend was greatly enhanced by fascin.

We found that quantitative differences among MSD distributions correlated with the type of F-actin microstructures and associated inhomogeneities present in the solutions. The MSD distribution of glycerol was symmetric with a

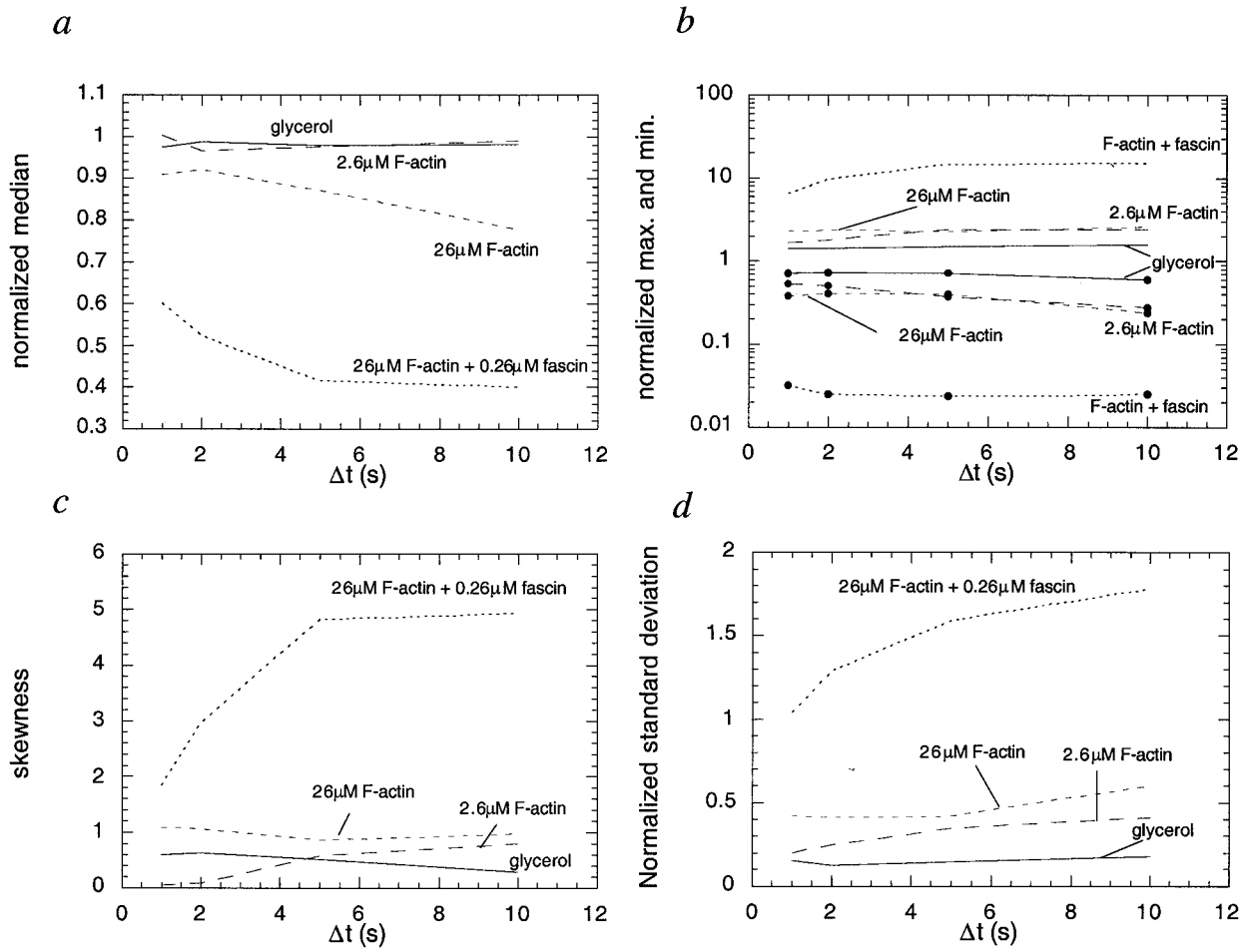

FIGURE 6 Time-scale-dependent median, minimum and maximum values, standard deviation, and skewness of the MSD distribution of microspheres suspended in glycerol, F-actin, and in an F-actin solution with fascin. MSD distributions are normalized by the ensemble-average MSD (see Fig. 3, *b*, *d*, and *f*) at each time scale and for each type of solution. (*a*) Median. (*b*) Maximum and mimum values of the MSD distribution. Circles correspond to minimum values. (*c*) Skewness. (*d*) Standard deviation.

standard deviation equal to that predicted for a perfectly homogeneous fluid at all tested time scales (Qian et al., 1991), whereas we found increased variations in MSD for increasing actin concentration. Following Onsager's classical predictions for the onset of liquid-crystal ordering in rigid-rod systems (Doi and Edwards, 1989; Morse, 1998a), semiflexible actin filaments will orient one another more readily at high actin concentration due to increased steric interactions. Indeed, F-actin forms a liquid crystal at concentrations as low as ≈50 μM (Kas et al., 1996), whereas pretransitional liquid-crystal domains are present at concentrations lower than 50 μM (Xu, 1997). The formation of these physical bundles (as opposed to chemical bundles, such as those formed by fascin), which are detected by confocal microscopy (Fig. 7) and polarized microscopy (Xu, 1997), create ordered structures in solution, which renders the actin solution relatively heterogeneous. These microstructural differences are reflected in the MSD distributions. At high F-actin concentration or in F-actin solutions with fascin, microspheres either become sterically trapped in bundle-rich and F-actin-rich regions of the solutions, or move relatively freely in actin-depleted regions. The first class of microspheres' displacements is much more densely populated than the second class. The existence of these two differently populated classes of microspheres, illustrated by the large variations in displacements (see Fig. 2, *c* and *c′*), leads to a highly asymmetric MSD distribution. Note that the displacements (≈10–50 nm, see *inset* in Fig. 4 *d*) of microspheres that belong to the first class (small-amplitude displacements) are still much larger than the spatial resolution of our MPT instrument (≈4 nm).

The standard deviation of the MSD distribution increases with time scale for both concentrated F-actin solutions and F-actin solutions in the presence of fascin. This may be explained by the fact that the beads that are allowed to move more freely (those that belong to the second class, see above) will increase their MSD over time. These beads are moving in a microenvironment, which is, from a rheological

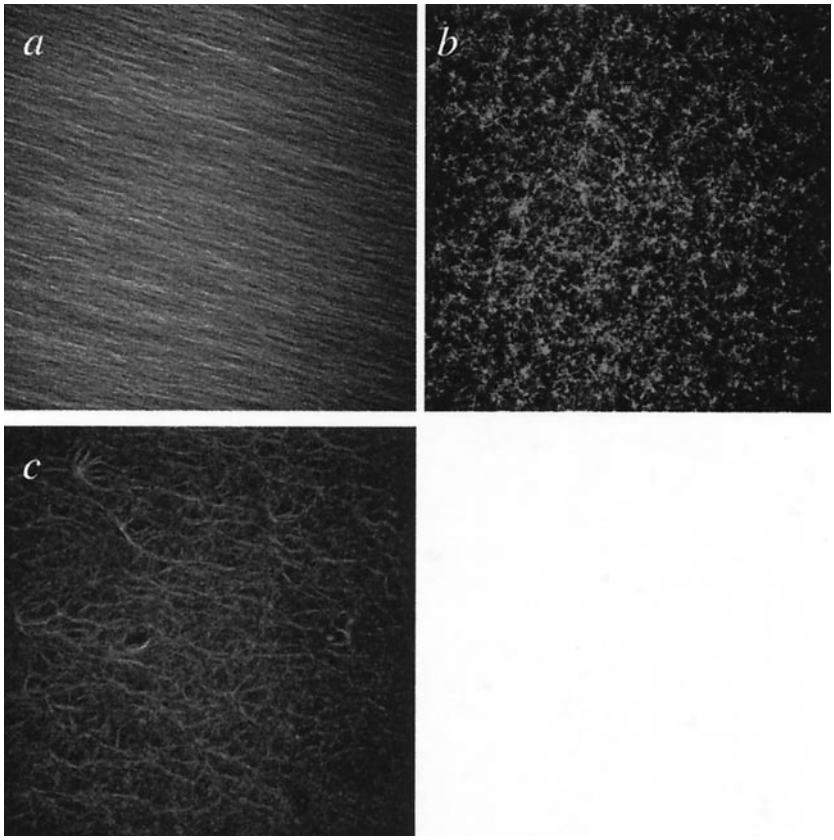

FIGURE 7 Confocal micrographs of solutions of rhodamine-labeled actin filaments in the presence or absence of human fascin. (*a*) 26 μM F-actin. (*b*) 2.6 μM F-actin. (*c*) 26 μM F-actin with 0.26 μM fascin. Scale bar, 5 μm.

point of view, relatively more liquid-like (Palmer et al., 1999; compare Fig. 1 *c* for the purely viscous liquid glycerol with the distribution of MSDs shown in Fig. 3 *e* for a viscoelastic solution). This interpretation is based on the quantitative relation between MSD and microrheology of polymer solutions, which has been confirmed for many systems (Palmer et al., 1999, 1998b; Xu et al., 1998c). In contrast, the MSD of microspheres whose motion is hindered by actin filaments and actin bundles reaches a plateau quickly as these beads experience a rheological microenvironment that is more solid-like (Palmer et al., 1999). Hence, the difference in MSD magnitudes between these two classes of microspheres increases with time, which in turn increases the standard deviation of the overall MSD distribution with time. As expected, more homogeneous solutions, such as glycerol and low-concentrated F-actin solutions, display MSD distributions that are only weakly dependent on timescale. Therefore the distribution of MSD, characterized by its width, skewness, and median, is an excellent marker of inhomogeneity in an F-actin solution.

Relation between F-actin organization in solution and F-actin rheology

Actin polymerization and gelation take place on very different time scales. At physiological concentrations of salt, a 26-μM G-actin solution polymerizes in $<$5 min (Korn et al., 1987). However, actin gelation, as probed by an increase of the elastic modulus, is extremely slow, as the stiffness of the same 26-μM actin solution takes $>$1 hour to reach a steady-state value (Xu et al., 1998a). Hence, contrary to the widespread assumption invoked in the falling-ball viscometric assay (Griffith and Pollard, 1982), the kinetics of actin gelation is not controlled by actin polymerization. Instead, we believe that the enormous time-scale discrepancy between polymerization kinetics and gelation kinetics is due to the (slow) establishment of a globally homogeneous F-actin network. Local heterogeneities (i.e., the presence of small and large pores) in the F-actin network represent defects that can transiently dominate the macroscopic mechanical properties of an F-actin network undergoing gelation, yielding a temporarily weak gel. Over time, actin filaments can diffuse into the large pores, which renders the mesh size uniform and, in turn, increases the overall stiffness. However, this homogenization process is slow because the movement of each actin filament in solution is constrained by surrounding filaments (Kas et al., 1996, 1994). We are currently testing this model of actin gelation using MPT.

We note that MPT requires small amounts (20–40 μl) of sample, which is particularly advantageous for protein samples. By comparison, DWS requires $\approx$0.3 ml (Palmer et al., 1998b,a) and conventional mechanical rheometers need

≈1.4 ml (Kas et al., 1996; Wachsstock et al., 1993; Ma et al., 1999). MPT described here complements traditional biophysical methods such as rheology, light scattering, microscopy, and spectroscopy to characterize the structural organization of concentrated actin filaments in vitro. These studies now provide the basis for extending the MPT method for the characterization of the relationship between filamentous structure, biophysical properties, and function in living cells.

We thank P. A. Coulombe, J. Xu, and S. Yamada for insightful discussions. D. W. acknowledges financial support from the Whitaker Foundation, the National Science Foundation (DMR9623972, CTS9812624, DB19729358, and CTS9625468), the National Aeronautics and Space Administration (NAG81377), and the Donors of the Petroleum Research Foundation administered by the American Chemical Society (32430AC7). S. C. A. acknowledges financial support from the National Institutes of Health (AI44417).

REFERENCES

Carlier, M. F., V. Laurent, J. Santolini, R. Melki, D. Didry, G. X. Xia, Y. Hong, N. H. Chua, and D. Pantaloni. 1997. Actin depolymerizing factor (ADF/cofilin) enhances the rate of filament turnover: implication in actin-based motility. *J. Cell Biol.* 136:1307–1322.

Clark, E. A., and J. S. Brugge. 1995. Integrins and signal-transduction pathways: the road taken. *Science.* 268:233–239.

Doi, M., and S. F. Edwards. 1989. The Theory of Polymer Dynamics. Clarendon Press, Oxford.

Edidin, M., S. C. Kuo, and M. P. Sheetz. 1991. Lateral movements of membrane glycoproteins restricted by dynamic cytoplasmic barriers. *Science.* 254:1379–1382.

Furukawa, R., and M. Fecheimer. 1996. The structure, function, and assembly of actin filament bundles. *Int. Rev. Cytol.* 175:29–90.

Gittes, F., and F. C. MacKintosh. 1998. Dynamic shear modulus of a semiflexible polymer network. *Phys. Rev. E.* 58:R1241–1244.

Gittes, F., B. Schnurr, P. D. Olmsted, F. C. Macintosh, and C. F. Schmidt. 1997. Microscopic viscoelasticity: shear moduli of soft materials determined from thermal fluctuations. *Phys. Rev. Lett.* 79:3286–3289.

Griffith, L. M., and T. D. Pollard. 1982. The interactions of actin-filaments with microtubule-associated proteins. *J. Biol. Chem.* 257:9143–9151.

Hall, A. 1998. Rho GTPases and the actin cytoskeleton. *Science.* 279: 509–514.

Hanein, D., N. Volkmann, S. Goldsmith, A. M. Michon, W. Lehman, R. Craig, D. DeRosier, S. Almo, and P. Matsudaira. 1998. An atomic model of fimbrin binding to F-actin and its implications for filament crosslinking and regulation. *Nat. Struct. Biol.* 5:787–792.

Hinner, B., M. Tempel, E. Sackmann, K. Kroy, and E. Frey. 1998. Entanglement, elasticity, and viscous relaxation of actin solutions. *Phys. Rev. Lett.* 81:2614–2617.

Hynes, R. O. 1989. Fibronectins. Springer-Verlag, New York.

Isambert, H., and A. C. Maggs. 1996. Dynamics and rheology of actin solutions. *Macromolecules.* 29:1036–1040.

Janmey, P. A. 1998. The cytoskeleton and cell signaling: vomponent localization and mechanical coupling. *Physiol. Rev.* 78:763–781.

Jones, J. D., and K. Luby-Phelps. 1996. Tracer diffusion through F-actin: effect of filament length and cross-linking. *Biophys. J.* 71:2742–2750.

Kas, J., H. Strey, and E. Sackmann. 1994. Direct imaging of reptation for semiflexible actin filaments. *Nature.* 368:226–229.

Kas, J., H. Strey, J. X. Tang, D. Fanger, E. Sackmann, and P. Janmey. 1996. F-actin, a model polymer for semiflexible chains in dilute, semidilute, and liquid crystalline solutions. *Biophys. J.* 70:609–625.

Konstantopoulos, K., and L. V. McIntire. 1996. Cell adhesion in vascular biology: effects of fluid dynamic forces on vascular cell adhesion. *J. Clin. Invest.* 98:2661–2665.

Korn, E. D., M. F. Carlier, and D. Pantaloni. 1987. Actin polymerization and ATP hydrolysis. *Science.* 238:638–644.

Kroy, K., and E. Frey. 1996. Force-extension relation and plateau modulus for wormlike chains. *Phys. Rev. Lett.* 77:306–309.

Kusumi, A., and Y. Sako. 1996. Cell surface organization by the membrane skeleton. *Curr. Opin. Cell Biol.* 8:566–574.

Lauffenburger, D. A., and A. F. Horwitz. 1996. Cell migration: a physically integrated molecular process. *Cell.* 84:359–369.

Leduc, P., C. Haber, G. Bao, and D. Wirtz. 1999. Dynamics of individual flexible polymers in a shear flow. *Nature.* 399:564–566.

Lee, G. M., F. Zhang, A. Ishihara, C. McNeil, and K. Jacobson. 1993. Unconfined lateral diffusion and an estimate of pericellular matrix viscosity revealed by measuring the mobility of gold-tagged lipids. *J. Cell Biol.* 120:25–35.

Luby-Phelps, K. 1993. Physical properties of cytoplasm. *Curr. Opin. Cell. Biol.* 6:3–9.

Luby-Phelps, K., P. E. Castle, D. L. Taylor, and F. Lanni. 1987. Hindered diffusion of inert tracer particles in the cytoplasm of mouse 3T3 cells. *Proc. Natl. Acad. Sci. USA.* 84:4910–4913.

Ma, L., J. Xu, P. A. Coulombe, and D. Wirtz. 1999. Epidermal keratin suspensions have unique micromechanical properties. *J. Biol. Chem.* 274:19145–19151.

Maciver, S. K., D. H. Wachsstock, W. H. Schwarz, and T. D. Pollard. 1991. The actin filament severing protein actophorin promotes the formation of rigid bundles of actin filaments crosslinked with alpha-actinin. *J. Cell Biol.* 115:1621–1628.

MacLean-Fletcher, S. D., and T. D. Pollard. 1980. Viscometric analysis of the gelation of acanthamoeba extracts and purification of two gelation factors. *J. Cell Biol.* 85:414–428.

Mason, T. G., A. Dhople, and D. Wirtz. 1997a. Concentrated DNA rheology and microrheology. *In* Statistical Mechanics in Physics and Biology. D. Wirtz and T. C. Halsey, editors. 153–158.

Mason, T. G., K. Ganesan, J. V. van Zanten, D. Wirtz, and S. C. Kuo. 1997b. Particle-tracking microrheology of complex fluids. *Phys. Rev. Lett.* 79:3282–3285.

Mason, T. G., and D. Weitz. 1995. Optical measurements of frequency-dependent linear viscoelastic moduli of complex fluids. *Phys. Rev. Lett.* 74:1254–1256.

McGough, A., W. Chiu, and M. Way. 1998. Determination of the gelsolin binding site on F-actin: implications for severing and capping. *Biophys. J.* 74:764–772.

McGowan, K., and P. A. Coulombe. 1998. Onset of keratin 17 expression coincides with the definition of major epithelial lineages during skin development. *J. Cell Biol.* 143:469–486.

Miki, H., T. Saski, Y. Takai, and T. Takenawa. 1998. Induction of filipodium formation by a WASP-related actin depolymerizing protein N-WASP. *Nature.* 391:93–96.

Milligan, R. A., and P. F. Flicker. 1987. Structural relationships of actin, myosin, and tropomyosin revealed by cryoelectron microscopy. *J. Cell Biol.* 105:29–39.

Mitchison, T. J., and L. P. Cramer. 1996. Actin-based cell motility and cell locomotion. *Cell.* 84:371–379.

Morse, D. C. 1998a. Viscoelasticity of concentrated isotropic solutions of semiflexible polymers. 1. Model and stress tensor. *Macromolecules.* 31:7030–7043.

Morse, D. C. 1998b. Viscoelasticity of concentrated isotropic solutions of semiflexible polymers. 2. Linear response. *Macromolecules.* 31: 7044–7067.

Morse, D. C. 1998c. Viscoelasticity of tightly entangled solutions of semiflexible polymers. *Phys. Rev. E.* 58:R1237–R1240.

Mullins, R. D., J. A. Heuser, and T. D. Pollard. 1998. The interaction of Arp2/3 complex with actin: nucleation, high affinity pointed end capping, and formation of branching networks of filaments. *Proc. Natl. Acad. Sci. USA.* 95:6181–6186.

Owen, C. H., D. G. Morgan, and D. J. DeRosier. 1996. Image analysis of helical objects: the Brandeis Helical Package. *J. Struct. Biol.* 116: 167–175.

Paladini, R., N. S. Bravo, K. Takahashi, and P. A. Coulombe. 1996. Onset of re-epithelialization after skin injury correlates with a reorganization of keratin filaments in wound edge keratinocytes: defining a potential role for keratin 16. *J. Cell Biol.* 132:381–398.

Palecek, S. P., A. Huttenlocher, A. F. Horwitz, and D. A. Lauffenburger. 1998. Physical and biochemical regulation of integrin release during rear detachment of migrating cells. *J. Cell Sci.* 111:929–940.

Palmer, A., B. Cha, and D. Wirtz. 1998a. Structure and dynamics of actin filament solutions in the presence of latrunculin A. *J. Polym. Sc. Physics Ed.* 36:3007–3015.

Palmer, A., J. Xu, S. C. Kuo, and D. Wirtz. 1999. Diffusing wave spectroscopy microrheology of actin filament networks. *Biophys. J.* 76:1063–1071.

Palmer, A., J. Xu., and D. Wirtz. 1998b. High-frequency rheology of crosslinked actin networks measured by diffusing wave spectroscopy. *Rheologica Acta.* 37:97–108.

Pelham, R. J., and Y. L. Wang. 1997. Cell locomotion and focal adhesions are regulated by substrate flexibility. *Proc. Natl. Acad. Sci. USA.* 94: 13661–13665.

Qian, H., M. P. Sheetz, and E. L. Elson. 1991. Single particle tracking: analysis of diffusion and flow in two-dimensional systems. *Biophys. J.* 60:910–921.

Sasaki, Y., K. Hayashi, T. Shirao, R. Ishikawa, and K. Kohama. 1996. Inhibition by drebrin of the actin-bundling activity of brain fascin, a protein localized in filopodia of growth cones. *J. Neurochem.* 66: 980–988.

Schnurr, B., F. Gittes, F. C. MacKintosh, and C. F. Schmidt. 1997. Determining microscopic viscoelasticity in flexible and semiflexible polymer networks from thermal fluctuations. *Macromolecules.* 30: 7781–7792.

Small, J. V., K. Rottner, and I. Kaverina. 1999. Functional design in the actin cytoskeleton. *Curr. Opin. Cell Biol.* 11:54–60.

Spudich, J. A., and S. Watt. 1971. The regulation of rabbit skeletal muscle contraction. *J. Biol. Chem.* 246:4866–4871.

Svitkina, T. M., and G. G. Borisy. 1999. Arp2/3 complex and actin depolymerizing factor cofilin in dendritic organization and treadmilling of actin filament array in lamellipodia. *J. Cell Biol.* 145:1009–1026.

Tamura, M., J. G. Gu, K. Matsumoto, S. Aota, R. Parsons, and K. M. Yamada. 1998. Inhibition of cell migration, spreading, and focal adhesions by tumor suppressor PTEN. *Science.* 280:1614–1617.

Tilney, L. G., M. S. Tilney, and G. M. Guild. 1995. F-actin bundles in drosophilia bristles. *J. Cell Biol.* 130:629–638.

Wachsstock, D., W. H. Schwarz, and T. D. Pollard. 1993. Affinity of α-actinin for actin determines the structure and mechanical properties of actin filament gels. *Biophys. J.* 65:205–214.

Xu, J., A. Palmer, and D. Wirtz. 1998a. Rheology and microrheology of semiflexible polymer solutions: actin filament networks. *Macromolecules.* 31:6486–6492.

Xu, J., W. H. Schwarz, J. Kas, P. J. Janmey, and T. D. Pollard. 1998b. Mechanical properties of actin filament networks depend on preparation, polymerization conditions, and storage of actin monomers. *Biophys. J.* 74:2731–2740.

Xu, J., V. Viasnoff, and D. Wirtz. 1998c. Compliance of actin filament networks measured by particle-tracking microrheology and diffusing wave spectroscopy. *Rheologica Acta.* 37:387–398.

Xu, J., D. Wirtz, and T. D. Pollard. 1998d. Dynamic cross-linking by α-actinin determines the mechanical properties of actin filament networks. *J. Biol. Chem.* 273:9570–9576.

Xu, J. Y. 1997. Ph.D. Dissertation, The Johns Hopkins University, Baltimore.

Yamada, S., D. Wirtz, and S. C. Kuo. 2000. Mechanics of living cells measured by laser tracking microrheology (LTM). *Biophys. J.* (in press).